Observation of Gentle Hump Structure on Energy Distribution Functions of End-Loss Ions in the rf-Driven Tandem Mirror Plasma

K. Ishii, T. Goto, Y. Goi, N. Kikuno, Y. Katsuki, M. Nagasaki, Y. Ono, N. Ishibashi, M. Yamanashi, M. Nakamura, I. Katanuma, A. Mase, M. Ichimura, A. Itakura, T. Tamano, and K. Yatsu

Plasma Research Center, University of Tsukuba, Ibaraki 305-8577 Japan

(Received 29 December 1998)

A gentle hump structure on energy distribution function of end-loss ions was observed in the rf-driven tandem mirror plasma by use of an end-loss energy component analyzer. Alfvén ion-cyclotron (AIC) fluctuations are excited spontaneously due to anisotropic ion heating in the central cell of the tandem mirror. We observed that the excitation of the AIC waves caused the hump structure on the energy distribution function. The enhancement factor of the end-loss ions is estimated, and the gentle hump structure is discussed from the viewpoint of the heating characteristics of the AIC waves. It is pointed out that the hump structure decreases the ion confinement.

PACS numbers: 52.55.Jd, 52.25.Fi, 52.70.Nc

In open systems, loss regions exist necessarily in the velocity space of the plasma. The plasma scattered from the trapped region to the loss region flows to the end walls along the magnetic field line. In order to improve the plasma confinement in the tandem mirror, the hyperboloidal loss boundaries in the velocity space are shifted in the direction of higher energy along a velocity component axis parallel to the magnetic field by creating electrostatic potentials on both sides of the plasma [1,2]. Effective plasma heating is also essential to achieve controlled thermonuclear fusion. Usually ions are heated anisotropically with respect to the direction of the magnetic field line, and various fluctuations are excited due to the anisotropic temperature. In the tandem mirror GAMMA 10 [3,4] ion-cyclotron-range-of-frequency (ICRF) waves are injected into the target plasma in the central cell. Ions are heated perpendicularly by the excited Alfvén slow waves [5]. At the same time, the Alfvén ion-cyclotron (AIC) fluctuations are also excited spontaneously in the central cell by reason of the anisotropic ion temperature [6]. The electromagnetic fluctuations cause diffusion of ions in the velocity space [7], therefore enhancement of the ion transport across the loss boundaries in the velocity space by carrying out the ion heating should be investigated on the same level as the effect of the electrostatic potential on the axial confinement in the tandem mirror. Here, we notice the hump structure on the energy distribution function of the end-loss ions in the rf-driven tandem mirror plasma and focus our discussion to the ion transport from the trapped region to the loss region caused by the AIC fluctuations. The energy and velocity distribution functions of the end-loss ions are measured by the end-loss energy component analyzer (ELECA) [8], and the AIC fluctuations are measured by reflectometers and magnetic probes. In this Letter, the energy flux is described briefly, next the observation of the hump structure is mentioned, and finally the mechanism of the hump structure and the influence of the hump on the ion confinement are discussed.

The tandem mirror GAMMA 10 consists of many mirror cells including a central cell, two anchor, and two plug/barrier cells. Figure 1 shows an axial profile of the magnetic field strength together with the locations of the main potential diagnostic devices and the rf antennas. The ELECAs are located at the positions of $z = \pm 13.6$ m. The ICRF waves are injected into the central cell to produce and heat the main plasma. Each mirror cell has the loss boundary which is characterized by both the magnetic mirror ratio and electrostatic potential produced in the plasma. Therefore, the boundary surrounding the loss region of the tandem mirror plasma is not necessarily a single hyperboloidal surface, and also the velocity distribution function in the loss region is far from a simple Maxwellian distribution, because the ions are heated locally and some of the trapped ions fall into the loss region from each mirror cell by pitch angle scattering caused by Coulomb collision and the interaction of particles with fluctuations.

We measured the energy distribution function $f_\epsilon(\epsilon)$ of the end-loss ions using the ELECA device [9], where ϵ is

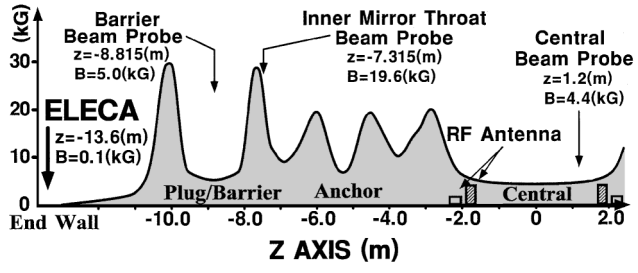

FIG. 1. Axial profile of the magnetic field strength is shown with the locations of the ELECA, beam probes, and ICRF antennas. The electrostatic potentials at the main parts are measured by the ELECA and the beam probes.

 0031-9007/99/83(17)/3438(4)$15.00

the ion energy. The $f_\epsilon(\epsilon)$ and the energy flux $F_{\epsilon\ \mathrm{loss}}$ are described as

$$f_\epsilon(\epsilon) = \frac{\sqrt{m}}{\sqrt{2}\, e\, \delta s R_A \sqrt{\epsilon^3}} \sum_{z_a=0}^{z_{\max}} 2\Delta I_s(\epsilon, z_a), \qquad (1)$$

$$F_{\epsilon\ \mathrm{loss}} = \frac{\sqrt{2}}{\sqrt{m}} \int d\epsilon \sqrt{\epsilon^3} f_\epsilon(\epsilon), \qquad (2)$$

where m is the ion mass, e is the unit charge, δs is the area of the small entrance aperture, R_A is the energy resolution of the ELECA, z_a is the position of the ion detector, $z_{\max}$ is the z_a coordinate of the small detector which detects the ion with the maximum pitch angle, and $\Delta I_s(\epsilon, z_a)$ is the ion current which enters the small detector located between z_a and $z_a + \Delta z_a$. The energy of ions can be analyzed from about 0.08 keV up to about 10 keV. The measured $f_\epsilon(\epsilon)$ is not necessarily simple even curves on a semilogarithmic scale. We observed that most of the $f_\epsilon(\epsilon)$ curves showed the gentle hump structure as shown in Fig. 2, where the background curve is estimated approximately as a summed up line of two types of straight lines in the semilogarithmic scale and plotted by small closed squares. The appearance of the hump structure depends on the ICRF heating conditions. Time evolution of the $f_\epsilon(\epsilon)$ curve with the sweeping time of about 1.5 msec is shown in Fig. 3 in two cases of experimental conditions: one is constant power injection of the ICRF wave, and the other is low power injection with adding subpulse of the ICRF wave in higher magnetic field configuration. In the upper figure, the hump structure appears almost constantly after realizing steady state, but in the lower figure the hump structure appears only during adding subpulse. The $f_\epsilon(\epsilon)$ curve at the time of 100 ms in the case of $B_0 = 4$ kG is plotted as closed circles in Fig. 4. In order to clear the hump structure, the difference of the intensity between the original curve of the $f_\epsilon(\epsilon)$ and the background curve is also plotted by open circles. Here we define an enhancement factor $g_{\mathrm{ehf(FWHM)}}$ as a ratio of the energy flux $F_{\epsilon\ \mathrm{loss(FWHM)}}$ of the original curve inside of the full width at half maximum (FWHM) of the gentle hump to the background energy flux $F_{\epsilon\ \mathrm{loss(FWHM)}}$(background) as follows:

$$g_{\mathrm{ehf(FWHM)}} = \frac{F_{\epsilon\ \mathrm{loss(FWHM)}}}{F_{\epsilon\ \mathrm{loss(FWHM)}}(\mathrm{background})}, \qquad (3)$$

$$F_{\epsilon\ \mathrm{loss(FWHM)}} = \frac{\sqrt{2}}{\sqrt{m}} \int_{\mathrm{inside\text{-}of\text{-}FWHM}} d\epsilon \sqrt{\epsilon^3} f_\epsilon(\epsilon).$$

The energy dependence of the enhancement factor is plotted in Fig. 5 under various heating conditions, and also the correlation between the normalized hump intensity ($g_{\mathrm{ehf(FWHM)}} - 1$) and the power of the AIC fluctuations are shown in Fig. 6 as an example. A remarkable feature is that trapped ions with characteristic energy flow selectively into the loss region so as to cause the gentle hump structure which appears in the energy region ($\sim$1.0–5.0) keV, and simultaneously excitation of the AIC fluctuations correlates strongly with the hump structure. The excitation of the AIC waves, which depends on the temperature anisotropy ($T_{i\perp}/T_{i\parallel}$) and plasma β values, have been already measured using reflectometers of microwaves and magnetic probes [6,10].

The mechanism of the hump structure on the $f_\epsilon(\epsilon)$ curve is considered at the points of the interaction with the AIC waves. The AIC waves excited with the anisotropic ion heating by the ICRF wave injection enhance the ion diffusion from the trapped region to the loss region. We consider the hump energy on the $f_\epsilon(\epsilon)$ curve from a viewpoint of ion trajectories in the ϵ-μ space induced by

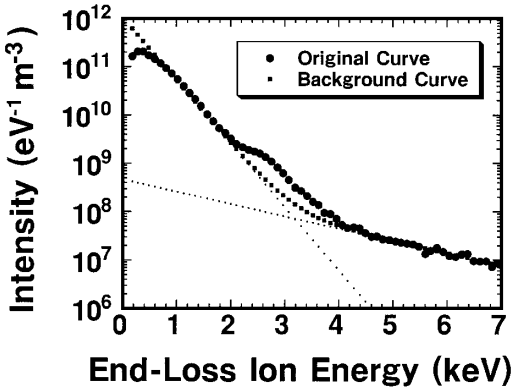

FIG. 2. Gentle hump structure on the energy distribution function $f_\epsilon(\epsilon)$. The structure appears in many $f_\epsilon(\epsilon)$ curves.

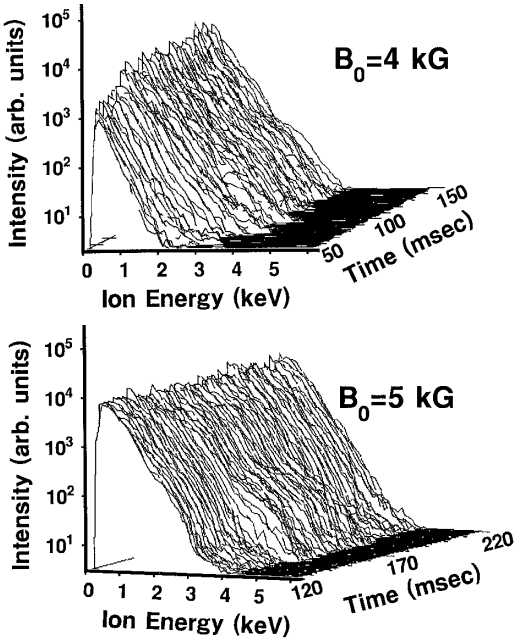

FIG. 3. Time evolution of the energy distribution function $f_\epsilon(\epsilon)$ in arbitrary units. The hump structure is observed clearly in different heating conditions. B_0 is the magnetic field at the midplane of the central cell.

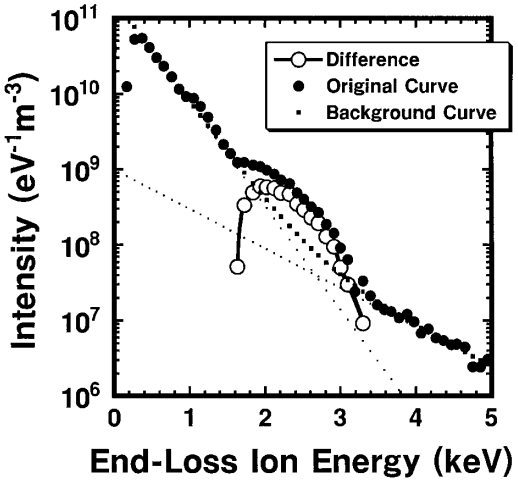

FIG. 4. An example of the hump structure. Open circles mean the enhanced energy distribution function which is obtained by subtracting the background curve from the original curve.

the cyclotron harmonic resonance due to small amplitude electromagnetic waves. The characteristic equation for the fundamental cyclotron resonance is described as follows by using the modified guiding-center differential equation [11]:

$$\mu = \left(\frac{\Omega_0}{B_0\omega}\right)\epsilon - C, \qquad C \geq 0, \tag{4}$$

where $\Omega_0 = eB_0/m$, B_0 is the magnetic field at the midplace, ω is the angular frequency of the wave, and C is constant. Using the parallel velocity component $v_{\parallel 0}$ and the perpendicular velocity component $v_{\perp 0}$ at the midplane, the equation is described as

$$\frac{v_{\parallel 0}^2}{(\frac{\Omega_0}{\omega} - 1)} + \frac{v_{\perp 0}^2}{(\frac{\Omega_0}{\omega})} = \frac{2B_0C}{(\frac{\Omega_0}{\omega})(\frac{\Omega_0}{\omega} - 1)m}. \tag{5}$$

As the angular frequency of the excited AIC wave is always lower than the ion-cyclotron angular frequency at the midplane of the central cell, for example, ω is $2\pi \times (6.95 \sim 7.25)$ MHz and Ω_0 is $(2\pi \times 7.76$ MHz) [10], the heating characteristic curves become ellipses. The ion-cyclotron resonance condition is $\omega - k_\parallel v_\parallel = \Omega$, where $k_\parallel$ is the parallel component of the wave number, $v_\parallel$ is the parallel velocity component, and Ω is the ion-cyclotron angular frequency. As the ELECA device used here is located at the position of $z = -13.6$ m, $v_\parallel$ is negative and $k_\parallel$ is positive. The low energy of the resonant particle is approximately restricted to $(m/2)\{(\Omega_0 - \omega)/k_\parallel\}^2$ because of $\Omega \geq \Omega_0$. The frequency and the parallel wave number are changed with the excitation condition, that is, temperature anisotropy and β values, and so on. We estimated the hump energy caused by typically excited AIC waves. For the estimation, we adopted the experimental results which were obtained by the simultaneous measurements of the ω and the $k_\parallel$ and the energy distribution function $f_\epsilon(\epsilon)$. The energy of the hump structure was estimated to be 1.6 and 2.5 keV for $\omega = 2\pi \times 7.11$ MHz, $k_\parallel = 8.8$ m^{-1} and $\omega = 2\pi \times 7.07$ MHz, $k_\parallel = 7.0$ m^{-1} [10], respectively. The results are in good agreement with the hump structure measurement. The electrostatic potential in the central cell of the tandem mirror GAMMA 10 is observed to be about 0.3 kV, and the entrance aperture of the ELECA is grounded, therefore the hump energy, which is measured by the ELECA, is added by about 0.3 keV. The gentle hump structure is distributed mainly over the energy region (~1.0–5.0) keV because of the variation of the frequency and the wave number.

Next, we consider another important process, that is, the ICRF waves cause the ion transport in the velocity space. In order to investigate the energy dependence of the ion flux which crosses the loss boundary in the velocity space, we took the ion influx from the trapped

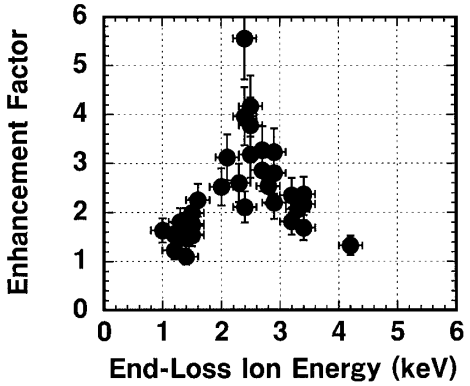

FIG. 5. Energy dependence of the enhancement factor. High enhancement factor is observed in the energy range of (~2.0–3.0) keV.

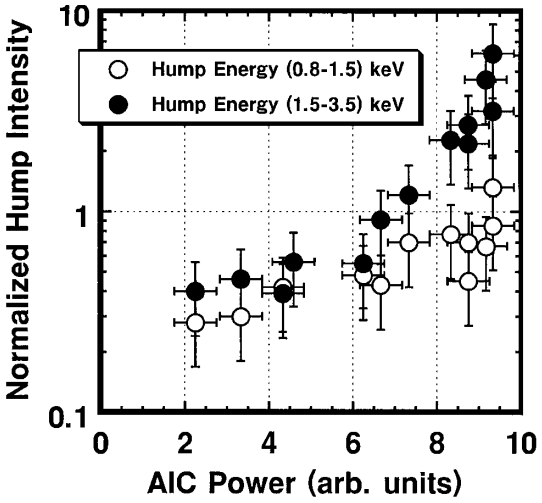

FIG. 6. Correlation between the normalized hump intensity and power of the AIC fluctuation. The power dependence in the energy range of (~1.0–1.5) keV is moderated as compared with the higher energy range.

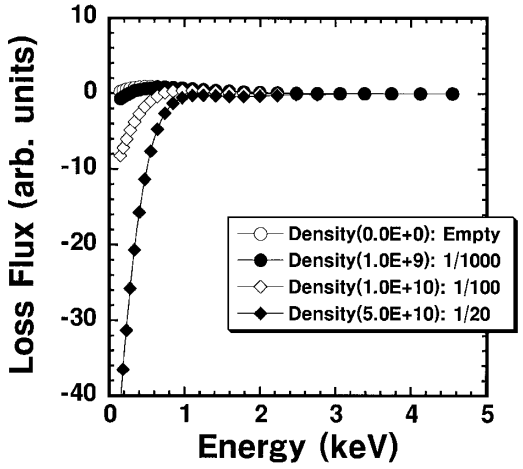

FIG. 7. The calculated loss flux is shown as a function of the ion energy on the condition that four kinds of ion densities are assumed in the loss region. The unit of the density is cm^{-3}.

region into the loss region due to the ICRF heating into consideration on the assumption that flow plasma exists constantly in the loss region in addition to the ion flux caused by the Coulomb collision, using a bounce averaged Fokker Planck equation [12]. The initial plasma with Maxwellian distribution is given in the trapped region, and also the Maxwellian flow plasma exists constantly in the loss region. We calculated the ion flux on the condition that the initial density of the plasma in the trapped region was 10^{18} m^{-3}, which was consistent with the experimental result; the densities of the flow plasma in the loss region were 0, 10^{15}, 10^{16}, and 5×10^{16} m^{-3}, and the frequency and the amplitude of the ICRF wave are 6.6 MHz and 0.3 $\mathrm{kV\,m}^{-1}$, respectively. The existence of the Maxwellian flow plasma in the loss region is not necessarily correct as the simulation model, but the simulation results are useful, because the density in the loss region approximately agrees with the density ($10^{15} \sim 5 \times 10^{16}$) m^{-3} estimated from the $f_\epsilon(\epsilon)$ measurement. In Fig. 7, the ion flux flowing into the loss region from the trapped region is plotted in arbitrary unit, which is proportional to $\sqrt{\epsilon}\, f_\epsilon(\epsilon) d\epsilon$. The simulated results are as follows: as the density of the flow plasma in the loss region increases, the low energy influx from the loss region into the trapped region increases rapidly, but the flux with the energy higher than about 1 keV is not much affected by the ICRF waves. We attend that in the energy range higher than about 1.5 keV the influence of the ion flow from the trapped region to the loss region on the $f_\epsilon(\epsilon)$ curve is almost negligible. We examined the tendency for the ion flux to change by varying the amplitude ($\sim$0.1–0.5) $\mathrm{kV\,m}^{-1}$ of the ICRF wave and the ion temperatures ($\sim$0.1–0.5) keV of the flow plasma, and confirmed that the tendency did not change significantly. Therefore, we conclude that the hump structure, which appears in the energy region ($\sim$1.0–5.0) keV, is caused by the excitation of the AIC waves, though we have to analyze carefully the hump structure for the energy region lower than about 1.5 keV. The hump structure is a significant phenomenon for reasons that the enhancement factor $g_{\mathrm{ehf(FWHM)}}$ corresponding to the energy more than 2.0 keV grows up to about 4 without difficulty, and the higher confining potential than the hump energy is required to confine the hump ions effectively.

The hump structure was observed on the energy distribution functions $f_\epsilon(\epsilon)$ of the end-loss ions by use of the ELECA device in the rf-driven tandem mirror plasma. It was found that the hump structure was caused by electromagnetic fluctuations of the AIC mode spontaneously excited by anisotropic ion heating. The enhancement factor $g_{\mathrm{ehf(FWHM)}}$ of the energy flux of the end-loss ion was estimated. Special attention should be paid to strong anisotropic ion heating for the open systems which contain necessarily the loss regions in velocity space, because the spontaneously excited AIC fluctuations enhance seriously the ion diffusion from the trapped region to the loss region.

The authors appreciate collaborations and discussions with members of the GAMMA 10 group of the University of Tsukuba.

[1] G. I. Dimov, V. V. Zakaidakov, and M. E. Kisinevskij, Sov. J. Plasma Phys. **2**, 326 (1976).
[2] T. K. Fowler and B. G. Logan, Comments Plasma Phys. Control. Fusion **2**, 167 (1977).
[3] M. Inutake *et al.,* in *Proceedings of the 3rd Technical Committee Meeting and Workshop* (IAEA, Tokyo, 1983), Vol. 1, p. 429 (Report No. IAEA-TC-392/25, 1983).
[4] M. Inutake *et al.,* Nucl. Fusion Suppl. **1**, 545 (1983).
[5] M. Ichimura *et al.,* in *Proceedings of the 14th EPS on Controlled Fusion and Plasma Physics* (EPS, Madrid, 1987), Vol. 11D, Pt. II, p. 554.
[6] M. Ichimura *et al.,* Plasma Phys. Controlled Fusion **34**, 1889 (1992).
[7] T. Tajima and J. M. Dawson, Nucl. Fusion **20**, 1129 (1980).
[8] K. Ishii *et al.,* Phys. Fluids B **4**, 3823 (1992).
[9] K. Ishii *et al.,* J. Phys. Soc. Jpn. **66**, 2224 (1997).
[10] A. Kumagai *et al.,* Jpn. J. Appl. Phys. **36**, 6978 (1997).
[11] T. D. Rognlien, Phys. Fluids **26**, 1545 (1983).
[12] I. Katanuma, Report No. KAKEN-84-002, 1984.